

Fabrication of SiC whisker reinforced Al₂O₃ composites

M. YANG*, R. STEVENS

School of Materials, Division of Ceramics, University of Leeds, Leeds LS2 9JT, UK

It is reported that SiC whiskers and alumina powder can be mixed in water medium when the whiskers are flocculated and the powder deflocculated, and that the composite slip can be cast to high green density. However, sintering of the composite to fully dense material was found to be difficult. The reasons were the formation of whisker networks and the development of the differential sintering stresses in the matrix around the whiskers. Hot pressing was subsequently employed, and the use of the computerized dilatometer allowed the establishment of a quantitative relationship of the densification rate with pressure, temperature and SiC whisker content. The present results help provide a useful basis for the effective design, development and fabrication of the whisker-reinforced ceramic composite.

1. Introduction

Processing of the SiC whisker-reinforced Al₂O₃ composite has been studied by several investigators [1-5]. Mixing of SiC whiskers with Al₂O₃ powder is difficult because the whiskers tend to form strong agglomerates and significantly reduce the packing efficiency of the composite. Wet processing is the most favoured of the many approaches used to achieve a homogeneous mixture of the whiskers and the matrix powder. However, the details of the mixing stage, reported in the literature, vary substantially. The methods used have appeared to be controversial and have given inconclusive results, such that the mixing conditions have not been conclusively established.

The sintering of the whisker-reinforced composite is of importance. Unfortunately, Porter *et al.* [4] stated that no densification occurred for the composite containing 15 vol % SiC whiskers sintered at 1550°C in vacuum for 30 min. Tieggs and Becher [6] used higher temperatures and only achieved 83% theoretical density for the Al₂O₃ composite with 10 vol % SiC whiskers, fired between 1700 and 1800°C. They managed to improve the final density with the aid of liquid-phase sintering additives.

In view of the difficulties encountered with pressureless sintering, hot pressing has been used to densify the composite. In this technique, the mixture of the whiskers and the powder is uniaxially pressed at pressures ranging from 20 to 70 MPa. High temperatures, in excess of 1750°C, are normally required to produce fully dense composites. It is perhaps due to the severity of the hot-pressing conditions and the complexity of the composite system that there are few references available in the literature regarding the role of temperature, pressure and SiC whisker content on the densification behaviour of ceramic composites.

This paper reports on the problems outlined above. The dispersing and mixing conditions of SiC whiskers

and Al₂O₃ powder were studied in some detail. The slip-casting process was used, and the cast compact sintered, when the microstructural evolution during sintering was followed. A hot-pressing kinetic study was performed using a computerized dilatometer to quantify the effect of the controlled processing parameters such as pressure, temperature and SiC whisker content on the densification rate of the composite. The results can serve as a useful basis for the effective design and development of the whisker-reinforced ceramic composite.

2. Experimental procedure

2.1. Raw materials

The Al₂O₃ powder used in the study was prepared from the precipitation of an aluminium alkoxide in order that the composition of the powder could be controlled with minimum impurities. The median grain size of the powder is approximately 0.5 µm, and the specific surface area is 8 m² g⁻¹. The chemical analysis of the powder is presented in Table I. Controlled amounts of Mg(NO₃)₂ · 6H₂O were introduced to the powder as a sintering additive by ball milling in isopropanol alcohol. The powder slurry was then dried and calcined at 550°C in air for 1 h decomposing the nitrate to MgO.

The SiC whiskers were supplied by the Nikkei Co. Ltd. Fig. 1 shows large agglomerates representative of the as-received whiskers taken as a random sample from a commercial batch of the whiskers. The diameter of the whiskers appears to be in the range 0.1 to 2 µm, and the length from 10 to 100 µm. X-ray diffraction indicates that the whiskers are β-SiC with a small amount of α-SiC also present.

2.2. Processing before firing

The pre-firing process started with the pretreatment of the SiC whiskers, which were initially leached in 10%

* Present address: School of Materials Science, University of Bath, Bath, UK.

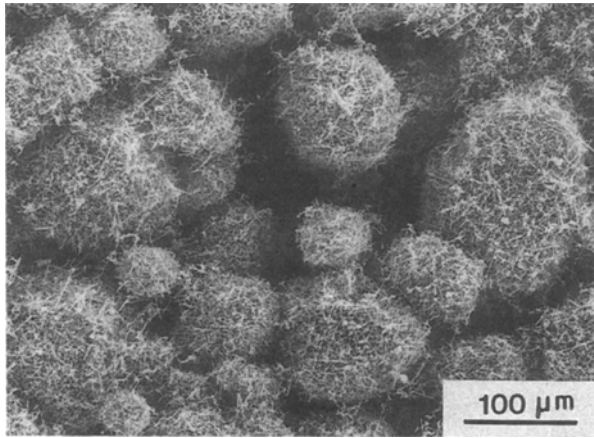


Figure 1 Scanning electron micrograph showing agglomerates of the as-received SiC whiskers.

HF solution to dissolve SiO_2 present on the surface of the whiskers. This was followed by washing five times with distilled water and drying on a hot plate at 60°C , after the whiskers had been filtered. The whiskers were weighed and added to excess distilled water, and were dispersed with an ultrasonic probe at pH 10 for 5 min. The whisker slurry was then flocculated at pH 2 and the water content was minimized after the whiskers settled down. Al_2O_3 powder was then introduced to the whisker slurry in the required amount. The mixture was vigorously blended using a high-intensity vibrational mixer and then further treated with an ultrasonic probe for 5 min. After being degassed, the blended slip was cast into a plaster mould. The slip was poured directly into the mould and drained after 15 min, when a layer of 5 mm was deposited. The cast specimen was dried in air and then in an oven at 110°C prior to sintering. The powder used for hot pressing was prepared by freeze drying.

2.3. Sintering

Oxidation of the SiC whiskers can take place at elevated temperatures in air, consequently the composite has to be sintered in a reducing atmosphere. A carbon bed was constructed which generated a reducing atmosphere to protect the SiC whiskers. Slip-cast compacts were placed in a graphite box, the box was embedded in a mixture of graphite and calcia-stabilized zirconia granules, which were, in turn, contained in a sealed alumina crucible. The whole assemblage was fired to 1600°C in an electric furnace with molybdenum disilicide heating elements.

2.4. Hot pressing

Hot pressing was carried out in an induction-heated graphite die. About 10 g powder was loaded into the die, which finally produced a 5 mm thick specimen. The powder was initially compacted at room temperature with a pressure slightly above that used at temperature. The pressure was then released to lower

TABLE I Chemical analysis of the alumina powder

	Impurity					
	Ca	Fe	Ge	Mg	Na	Si
Content (p.p.m.)	3	5	2	3	25	3

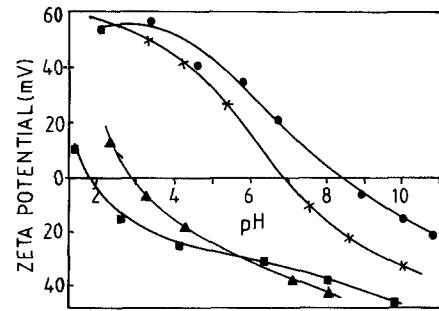


Figure 2 Zeta potential of the (■) SiC whiskers and (●) alumina plotted against pH. Other results (x) Sacks *et al.* [5] (▲) Lundberg *et al.* [2].

the die assembly, leaving a 1.5 mm gap on the top. For the kinetic study, pressure was applied after the sample was heated to the required temperature. When no further densification occurred within 200 sec, the hot pressing was terminated. The procedure changed slightly when the objective of the hot pressing was to attain high density. Two-thirds of the required pressure was applied at 1000°C and the full pressure used at the set temperature. The hot-pressing time varied from 30 to 60 min.

2.5. Density measurement

The density of green compacts and poorly sintered composites was measured by the mercury displacement method on a Doulton densometer. Dense composites were measured using the water displacement method, a few drops of wetting agent being added to the distilled water to ensure the penetration of small pores. Fine fishing thread was used to suspend the specimen. The accuracy of this method was estimated to be within 0.01 g cm^{-3} .

3. Results and discussion

3.1. Dispersion of the SiC whiskers and Al_2O_3 powder

Three separate stages are involved in the process of dispersing a dry powder in a liquid medium. Firstly, the dry powder should be wetted properly, such that there is a direct contact between the liquid medium and solid interface. Secondly, mechanical energy is required to break down agglomerates and to disperse the solid particles throughout the liquid medium. Finally, the dispersed state has to be maintained, because the particles have the natural tendency to agglomerate due to a combination of the Brownian motion and Van der Waals attractive forces. To counteract these attractive forces, repulsive forces are required and this is usually achieved through either electrostatic and/or steric interaction between particles.

In the present study, only the electrostatic approach was used and this is illustrated in terms of zeta potential. Fig. 2 shows the zeta potential of the Al_2O_3 powder and SiC whiskers in the water medium at different pH values. The Al_2O_3 particles are positively charged in the acidic medium and have the highest zeta potential of 60 mV at pH 3 with an isoelectric point at pH 8.5. The alumina powder could be readily dispersed at pH 3 when a maximum solids content of 72% was achieved. The viscosity of the alumina slip against pH values is plotted in Fig. 3. The results

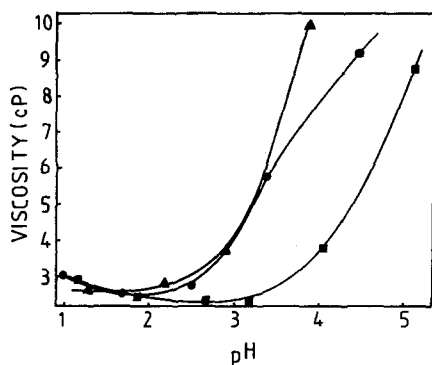


Figure 3 Viscosity of the alumina-SiC whisker composite slips plotted against pH. (■) Alumina slip, (●) C10 slip, (▲) C20 slip.

imply that the viscosity of the slip system is highly sensitive to pH. At a pH above 4, with the zeta potential less than about 50 mV, the viscosity of the slip increases dramatically. A plausible explanation is that once the potential is less than a critical value, the attractive forces described earlier exceed the repulsive forces and cause the coagulation of small particles. This deduction is supported by Adams [7] who predicted theoretically that 50 mV of surface potential was required to provide a barrier adequate to resist aggregation of a pair of 1 μm diameter particles of Al_2O_3 .

The SiC whiskers were found to be negatively charged over a wide range of pH values with a low isoelectric point, and the absolute potential increases with pH. This result coincided with a result of the sedimentation experiment. Fig. 4 represents the histogram of the sedimentation height of the SiC whiskers in water. In the acidic medium, the whiskers settled down rapidly in bulk, leaving a clear supernatant solution above them. The final sediment was loosely packed with a large specific volume and was easily redispersed, which suggested that the whiskers were flocculated. In contrast, in the basic suspension, the whiskers settled down slowly with a cloudy solution at the top and a densely packed layer at the bottom, indicating that the whiskers were deflocculated.

The zeta potential for the SiC whiskers reported in the literature has varied considerably. Lundberg *et al.* [2] found that the Tokai SiC whiskers had an isoelectric point at pH 3. Sacks *et al.* [5] recently obtained an isoelectric point at pH 7 for the Teteho SiC whiskers. Both these data are replotted in Fig. 2 and compared with the present result. The variation in the isoelectric point is not unexpected, and could well be caused by

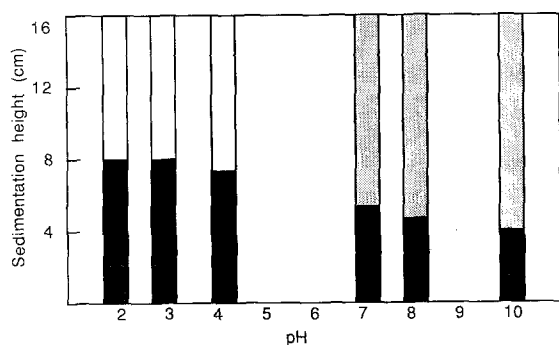


Figure 4 Histogram of the sedimentation characteristics of SiC whiskers at different pH values.

the presence of impurities together with SiO_2 on the surface of the whiskers.

The whiskers had to be dispersed in excess water. Intense ultrasonic treatment was found to be sufficient to cause separation of the as-received tangled whiskers at pH 10. The dispersed whiskers were then flocculated at pH 2 and mixed with Al_2O_3 powder.

3.2. Mixing of the SiC whiskers and Al_2O_3 powder

Several techniques were employed to blend the whiskers and the matrix powder. The effectiveness of these techniques was determined by dispersing an agglomerated powder which was calcined from the fine alumina powder at 800°C for 4 h. It was found that the powder was better dispersed by both the ultrasonic method and the agitation mixer, but that the former method yielded a higher proportion of small particles. Accordingly, the mixture of the SiC whiskers and Al_2O_3 powder was initially processed at pH 2 using the agitation mixer and further treated with the ultrasonic probe. The solid content and mixing time are a function of the whisker content in the composite, and these are listed in Table II.

The shape of the whiskers affected the total solid content in the slip which could be dispersed and this decreased sharply with the increase in whisker content. Mixing also became difficult when whisker content increased, a longer processing time being required. The viscosity of the resultant slips was measured using a Brookfield viscometer, and the results can be seen in Fig. 3. The slips were fluid only at a pH less than 3.0, beyond which the Al_2O_3 particles were neutralized by the oppositely charged SiC whiskers, causing heavy flocculation. The slip was stable in the fluid region such that little or no sedimentation and separation could be seen 5 h after the processed slip was left to stand. The uniformity of the slip, dispersed in the manner described, can be observed on the polished surface of the hot-pressed composite with 30 vol % SiC whiskers, as shown in Fig. 5. The SiC whiskers appear as the brighter phase due to their high optical reflectivity.

An important concept implied by this result is that a fluid and stable slip of the mixture of two phases can be achieved under the conditions when the major phase is deflocculated and the minor phase flocculated. A possible explanation is that the flocs of the whiskers can be redispersed and mixed uniformly with the matrix powder using a high-intensity mixer; the fluidity of the resultant slip is determined by the overall zeta potential of the system, and the relative stability provided by the network of the flocculated whiskers.

TABLE II Variation of solid content, mixing and dispersing time with SiC whisker volume fraction

	Material designation			
	C0	C10	C20	C30
SiC whisker content (vol %)	0	10	20	30
Total solid content in the slip (wt %)	72	68	60	50
Time for agitation mixing (h)		1	2	3
Time for ultrasonic treatment (min)		5	5	5

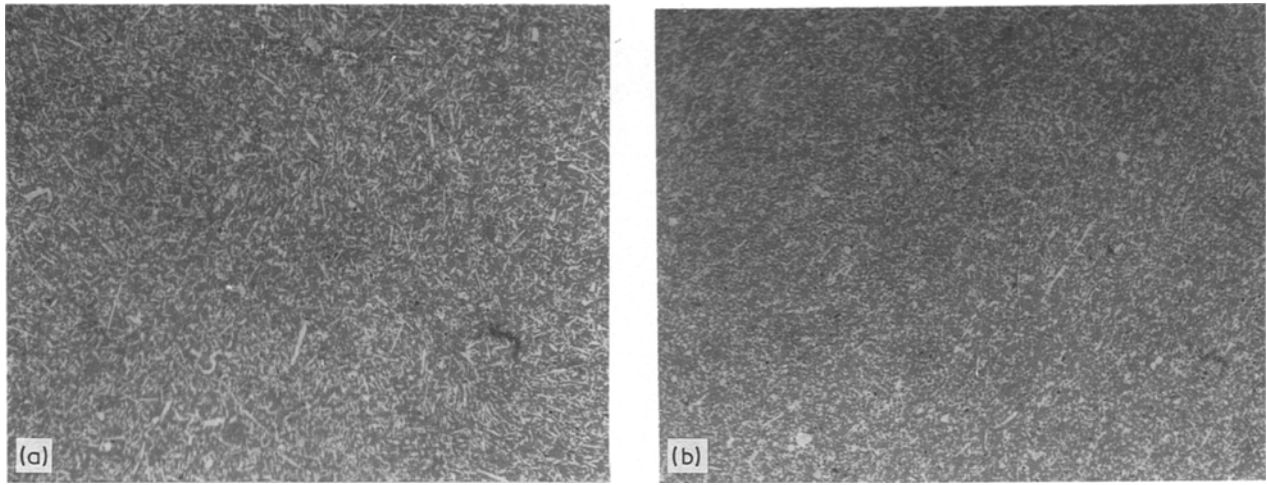


Figure 5 Optical micrographs of the polished surface of the hot-pressed composites containing 30 vol % SiC whiskers ($\times 250$): (a) parallel to the hot-pressing plane, (b) normal to the hot-pressing plane.

3.3. Consolidation

The composite slips were cast into plaster moulds. By varying the mixing time, a series of microstructures of the cast composite with 20 vol % SiC whiskers were produced and can be seen in Fig. 6. Large pores with whisker agglomerates were observed after 1 h of agitation mixing and 5 min ultrasonic dispersing, as shown in Fig. 6a, which apparently resulted from insufficient mixing. Further blending for another hour brought about a uniform distribution of the whiskers throughout the matrix. However, numerous small pores were still present (Fig. 6b) and these were associated with air bubbles introduced during vigorous mixing. Consequently, the slip was degassed prior to casting, and the resultant microstructure is illustrated in Fig. 6c. This shows a uniform microstructure with the whiskers having an average length of about $20\ \mu\text{m}$, which suggests that the breakage of the whiskers is minimal during mixing. A closer inspection indicates that the whiskers appear to be randomly orientated in the matrix, Fig. 8b.

The green density of the cast composite is given in Table III. A slight decrease in density with the increased whisker content is anticipated. Porter *et al.* [4] employed the pressure infiltration method to consolidate the composite slip with 15 vol % SiC whiskers. They achieved a green density in the range of 59% to 65% by varying the consolidation pressure from 0.78 to 7.8 MPa. Sacks *et al.* [5] ground the Teteho SiC whiskers to an average length less than $10\ \mu\text{m}$ and then mixed them with submicrometre alumina powders. They were able to achieve 67%

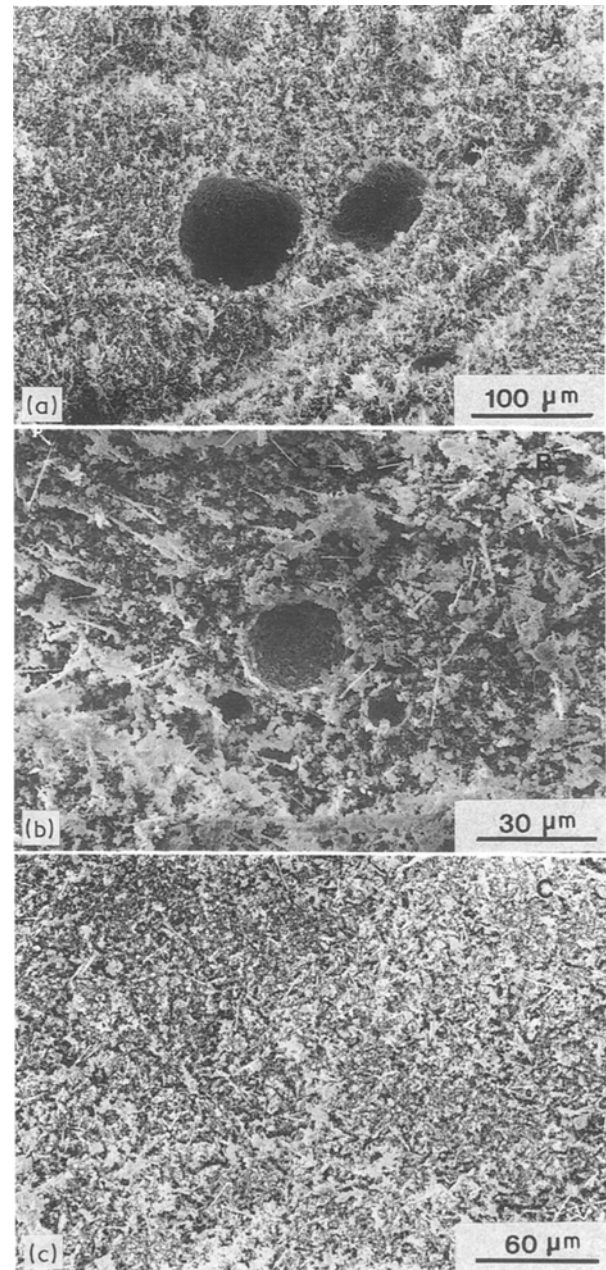


Figure 6 Microstructures of the slip-cast composite containing 20 vol % SiC whiskers, (a) after 1 h vibrational mixing and 5 min ultrasonic treatment, (b) after 2 h vibrational mixing and 5 min ultrasonic treatment, (c) after degassing.

TABLE III Sintered density of the composites

SiC whisker content (vol %)	Green density*	Density sintered at 1400°C^*	Density sintered at 1600°C^*	Density sintered at 1600°C
0	68	91	100	100
5	66	81	90	97
10	65	75	85	97
15	62	74	83	96
20	62	73	80	95

* Measured by mercury displacement method.

† Measured by water displacement method.

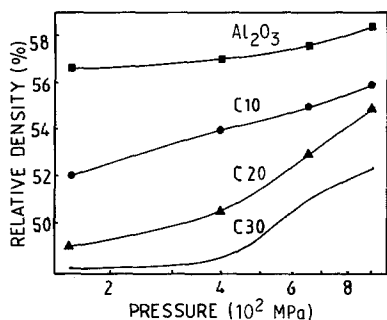


Figure 7 Die-pressed density of the composite plotted against applied pressure.

relative density for the whisker content up to 30 vol %. This suggests that shorter whiskers result in a higher packing efficiency for the whisker composites.

The effect of pressure on the relative density of the die-pressed compact is illustrated in Fig. 7. It can be seen that the packing density of the Al₂O₃ powder is relatively insensitive to the pressure, and that the packing density of the composite is substantially reduced with the increasing SiC whisker content and is clearly dependent on the applied pressure. At 10 vol % SiC whisker content, the increase of the density is approximately linear with log pressure. At 30 vol % SiC whiskers, the packing behaviour of the composite exhibits a transition. Little increase in density was observed in the pressure range 25 to 50 MPa; subsequently the density increased sharply with the pressure. This phenomenon can be related to the formation of the whisker network. The yielding stress of this network is suggested to be near 50 MPa, above which pressure the network breaks down, thereby causing further particle rearrangement and densification. In comparison, the green densities of the die-pressed compacts are at least 10% below those for the slip-cast green compacts of the same composition.

3.4. Sintering and microstructural evolution

The whiskers used in the present study have an elongated shape with diameters similar to those of the matrix particles. During the sintering process the matrix densifies by means of diffusion-controlled mechanisms; however, the shrinkage of the matrix particles in the vicinity of the whiskers is inhibited by the need for extensive sliding along the whisker boundary. Densification of the matrix is thus retarded by the drag force imposed by the whiskers.

Sintering becomes more difficult with the increasing whisker content because the whiskers are more likely to be in contact with each other, forming a rigid network. Zellen [8] determined experimentally the volume fraction for randomly dispersed inclusions at which a network can be formed. He mixed conductive and non-conductive particles of the same size and found that the mixture started conducting when the volume fraction of the conductive phase was at 0.16, which suggested that a continuous network of the conductive phase must have been present. The volume fraction of whiskers required to form a network is likely to be lower as a consequence of the high aspect ratio.

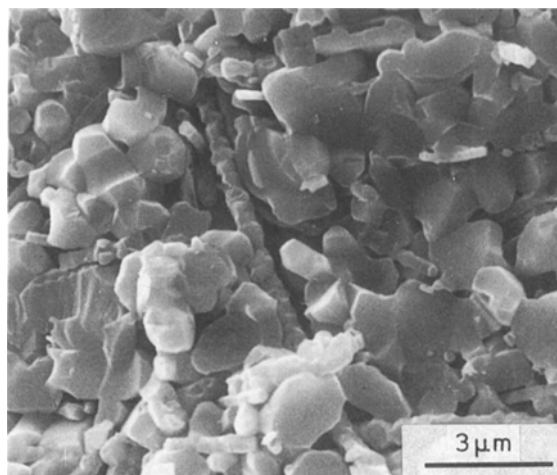


Figure 8 Microstructure of the C10 composite sintered at 1600° C for 5 h.

In the present investigation, the slip-cast composites were sintered at 1400 and 1600° C, respectively, for 5 h at a heating and cooling rate of 600° C h⁻¹. The density of the sintered composites containing 0 to 20 vol % SiC whiskers is shown in Table III. The unadulterated alumina powder doped with 300 p.p.m. MgO could be sintered to the theoretical density at 1500° C in 2 h. With the addition of whiskers into the matrix, the final density dropped rapidly, then levelled off at the whisker content above 10 vol %. This may be explained in that at low concentrations of less than 10 vol %, the whiskers in the matrix are separated, the decrease in densification is caused mainly by the differential sintering stresses associated with these whiskers. At high concentrations above 10 vol %, the whiskers are in contact with each other and form networks as indicated by Zellen's observations, such that densification rate is further impaired by these networks. It is believed that the latter phenomenon has a more deleterious effect on densification than the former. Once the network is formed, homogeneous densification is likely to cease completely.

Several characteristic defects present in the sintered composites were identified, which help explain how the whiskers inhibited the densification process. Fig. 8 shows the microstructure of the C10 composition sintered at 1600° C for 5 h. Matrix grain growth was extensive and the large whisker crossing the matrix appears to be disturbed, which may be caused by the differential sintering stresses developed along the length of the whisker. The elastic energy of the whisker might, in turn, have acted to resist densification. A large void space is clearly visible along the perimeter of the whisker. Fig. 9 illustrates a typical network formed by several whiskers. The large matrix grains, situated at the intersection of the whiskers, weld the network firmly, leaving interparticle voids. The fine particles present in the interstices of the network may sinter together. However, this internal shrinkage will not be reflected in the shrinkage of the composite as a whole. Hence, once the rigid whisker network is formed, densification becomes slow and attaining a high density becomes impossible.

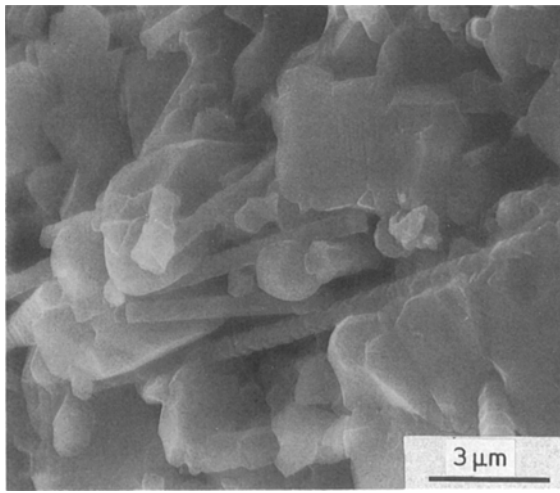


Figure 9 Microstructure of the C20 composite sintered at 1600°C for 5h.

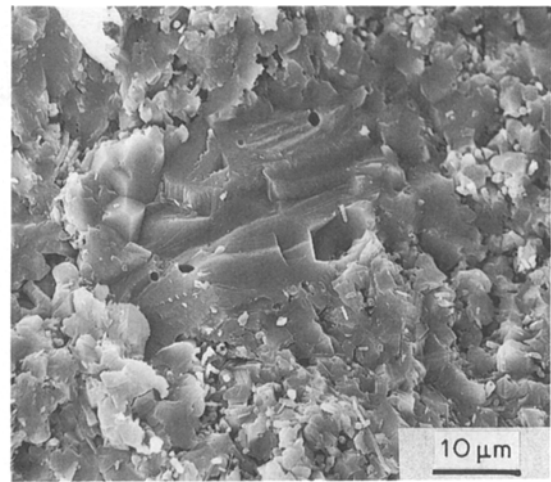


Figure 11 Fracture surface of the C20 composite (hot pressed at 1750°C, 27 MPa, 60 min, without MgO additive) containing large grains and pores adjacent to the grains.

3.5. Hot-pressing study

3.5.1. Determination of the optimum MgO addition

The C20 composite was chosen as an example and hot-pressed under the conditions of 1750°C, 27 MPa, 60 min. The effect of MgO on the final density is shown in Fig. 10. The density of the composite increased linearly with MgO content, and reached a maximum at 800 p.p.m., precisely at the solubility limit predicted by Roy and Coble [9].

The effect of MgO addition on the densification of Al₂O₃ has been exploited extensively. Several explanations are possible. Firstly, it is believed that MgO is dissolved in Al₂O₃ and forms a solid solution, which results in a defect structure with interstitial Al³⁺ ions, thereby increasing the Al³⁺ ion diffusivity. Because the Al³⁺ ion-diffusion rate is considered to be the rate-controlling process in the densification process, the ratio of densification rate to the grain growth will be enhanced. This enables densification to be achieved prior to substantial grain growth, and any grain growth to be restricted to the substantially densified body. Secondly, the presence of MgO dopant effectively avoids exaggerated grain growth. This is presumed to have been achieved by raising the pore mobility at grain boundaries [10].

Examination of the microstructure of the composite lends support to such explanations. Fig. 11 shows the fracture surface of the hot-pressed composite without MgO dopant. It can be seen that exaggerated grain

growth of the alumina had occurred. The large dense grains prevented the applied pressure being transmitted to the adjacent regions, thus inhibiting densification, typified by the presence of the surrounding pores. Intragranular pores are also visible in such large grains. In contrast, the microstructure of the composite doped with 800 p.p.m. MgO, as shown in Fig. 12, appears to be dense and uniform.

A further point verified from the above observation is that the optimum amount of the MgO dopant is determined by the solubility of MgO in Al₂O₃ at the densification temperature. This effect has also been observed in several previous studies. Peelan [11] stated that a maximum density of Al₂O₃ could be achieved at the sintering temperature of 1630°C with 300 p.p.m. MgO. Harmer [12] reported that a maximum densification rate could be obtained using hot pressing at 1630°C and 10 MPa with 300 p.p.m. MgO, which is just at the solid solution limit at this temperature. The amount of MgO required at other temperatures can be estimated; 350 p.p.m. MgO is suggested at 1650°C, and 1150 p.p.m. MgO at 1800°C.

The hot-pressed density of the composite doped with the optimum amount of MgO is listed in Table IV

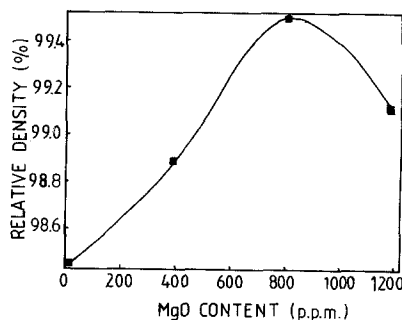


Figure 10 Effect of MgO addition on the final density of the hot-pressed composites.

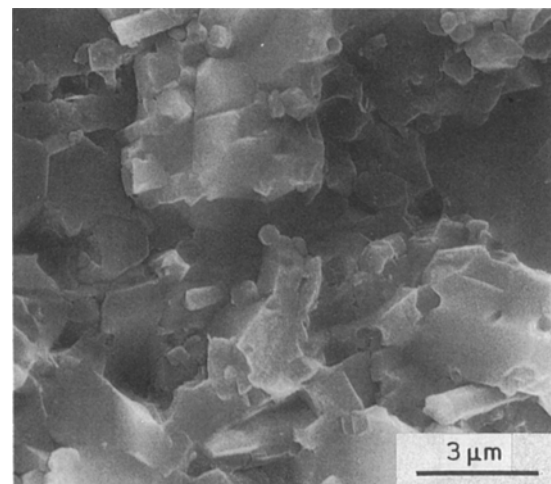


Figure 12 Fracture surface of the C20 composite hot pressed at 1750°C, 27 MPa, 60 min with MgO additive.

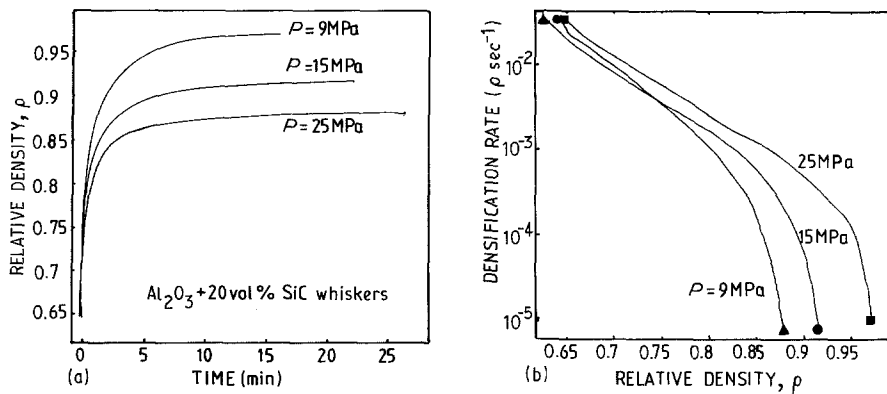


Figure 13 (a) and (b) Densification kinetics of the C20 composite hot pressed at 1750°C and various pressures.

along with the hot-pressing conditions. The microstructure of the C30 composite shown in Fig. 5 suggests that the whiskers have been preferentially aligned perpendicular to the stress axis.

3.5.2. Dependence of the densification rate on pressure

Coble and Spriggs [13] have suggested that there are two major mechanisms involved in hot pressing, namely plastic flow and stress-induced diffusion. In the initial stage of hot pressing, the plastic flow mechanism is dominant and densification is largely achieved by sliding and rearrangement of particles under the action of the applied pressure. The process is accompanied by particle fragmentation and is further increased by enlargement of the contact area of the particles, so that this stage has a strong resemblance to the mechanism taking place in die pressing. In the intermediate and late stages of hot pressing, densification is controlled by a stress-induced diffusion mechanism. The diffusion of the controlling species is accelerated by the applied pressure.

In the present study, the C20 composite doped with 800 p.p.m. MgO was hot pressed at 1750°C using a series of pressures. The densification kinetics data are presented in Fig. 13. The density-time curves show that the starting density of the composite increases slightly with applied pressure and that the final density rises with pressure from 90.2% at 10 MPa to 97.1% at 25 MPa. The densification rate-density curves indicate that the difference in the densification rate in the pressure range 10 to 25 MPa is small in the early stages of hot pressing, but becomes more pronounced during the intermediate and final stages.

The densification behaviour of the composite in the early stages of hot pressing is similar to the

compaction of the die-pressed composite discussed previously. At pressures below the yielding stress of the whisker network, the sliding and rearrangement of particles is inhibited so that the increase of densification rate with pressure is limited. With the increase of density and grain size, the whisker network becomes more rigid when the densification decreases dramatically. A high density is difficult to achieve, unless a very high pressure is applied, because the voids present in the interstices of the network tend to be beyond the size which can be removed by mass transport. This may well explain why densification virtually ceased at a relative density of 90.8% at 10 MPa.

In order to elucidate the mechanism of densification in the intermediate stage of hot pressing, the instantaneous densification rate at relative densities of 0.75%, 0.80% and 0.85% was determined and plotted against the applied pressure, Fig. 14. The straight lines were fitted to the data points according to the least squares method. At densities of 85%, the densification rate plotted with pressure assumes a linear relationship, indicative of densification being controlled by a diffusion creep mechanism. The data can be interpreted by the Nabarro-Herring [14] creep model if the diffusion process occurs through the lattice.

$$\frac{1}{\rho} \frac{d\rho}{dt} = \frac{40D_L\Omega}{3KTG^2} \sigma_{\text{eff}}$$

On the other hand, if the diffusion step is along the grain boundary, the Coble [15] creep model can be applied

$$\frac{1}{\rho} \frac{d\rho}{dt} = \frac{47\theta D_b\Omega}{KTG^3} \sigma_{\text{eff}}$$

where $(1/\rho)(d\rho/dt)$ is the relative densification rate,

TABLE IV Hot-pressing conditions and densities

Composition	Hot-pressing conditions			Relative density (%)
	Temp (°C)	Pressure (MPa)	Time (min)	
C10	1500	20	30	99.9
C20	1600	20	60	96.4
	1700	20	60	97.7
	1700	27	60	98.8
	1750	27	60	99.5
C30	1700	27	60	97.5
	1800	27	60	98.5

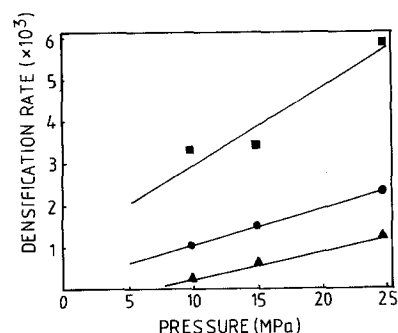


Figure 14 Plot of densification rate at $\rho =$ (■) 0.75, (●) 0.8, (▲) 0.85 against pressure.

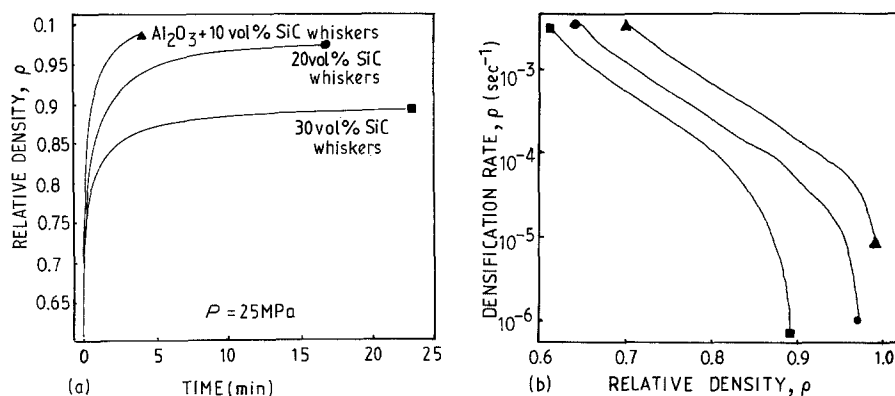


Figure 15 (a) and (b) Densification kinetics of the composites with 10 to 30 vol% SiC whiskers, hot pressed at 1750°C, 25 MPa.

K is the constant ($1.38 \times 10^{-16} \text{ erg K}^{-1}$), Ω is the volume of the oxide transported per Al^{3+} ion which is calculated to be $2.258 \times 10^{-29} \text{ cm}^3$, σ_{eff} is the applied pressure and D_L , ∂D_b are the lattice and grain-boundary diffusion coefficients respectively, which were calculated from the equation proposed by Cannon and Coble [16] for the MgO-saturated Al_2O_3 : at 1750°C $D_L = 1.76 \times 10^{-10} \text{ cm}^2 \text{ sec}^{-1}$, $\partial D_b = 1.41 \times 10^{-14} \text{ cm}^3 \text{ sec}^{-1}$.

Applying these data into both of the models with $\sigma_{\text{eff}} = 25 \text{ MPa}$ and $\rho = 0.85$, the grain size estimated from the Nabarro–Herring model is $1.91 \mu\text{m}$ and that from the Coble model is $4.67 \mu\text{m}$. The actual grain size appears to be around $2 \mu\text{m}$. This may suggest that densification was mainly contributed by the grain-boundary diffusion mechanism. However, the absence of the systematic experimental data on the dependence of the densification rate on the grain size does not allow for further speculation.

3.5.3. Dependence of densification rate on SiC whisker content

The composites with 10 to 30 vol% SiC whiskers were hot-pressed at 1750°C and 25 MPa. The densification kinetic data are presented in Fig. 15. The starting density of the composite increases with increasing whisker content. The C30 virtually ceased densification at a relative density of 91.8% after 45 min.

Table V shows the density of the C20 and C30 prepared by applying the pressure at the set temperature, after alignment at 1000°C. There is little difference for the composite with 20 vol% SiC whiskers. However, the advantage gained by applying pressure at low temperature is evident for the composite with 30 vol% SiC whiskers. The reason behind this action is again the requirement to achieve substantial densification before grain growth, and hence to prevent the formation of the rigid whisker network

in order that the residual porosity might be eliminated by the stress-induced diffusion mechanisms.

Fig. 16 shows the log densification rate at various densities plotted against SiC whisker content. The straight lines were again fitted to the data points using the least squares method. It appears that $\log \rho$ decreases linearly with the increasing SiC whisker content at a density of 0.75 and 0.80. An empirical expression can thus be proposed as follows

$$\log \rho = -kC + \text{const.}$$

where k is the slope of the straight lines and is calculated to be 0.4 at the relative density of 0.80, and C is the whisker volume fraction. The equation can be converted in an exponential form

$$\rho = 10^{-kC}$$

The constant k is a function of the aspect ratio of the whiskers, and may also change during the course of densification, as indicated by the different slopes at three different densities. The densification rate is expected to decline with the whisker content as a consequence of the exponential relationship. Because of the lack of the extensive experimental data, this dependence needs to be investigated further.

4. Conclusions

1. The alumina powder and SiC whiskers can be mixed in the water medium at pH 2 when the alumina is deflocculated and the whiskers flocculated. The agitation mixer, assisted by the ultrasonic probe, can blend the two phases uniformly. The mixed slip is fluid and stable, and can be cast to high green density.
2. Sintering of the whisker composite to high density is difficult, and may be even impossible. This is due to the differential sintering stresses and the formation of a whisker network.
3. Hot pressing is believed to be necessary to densify

TABLE V Comparison of the density of the composites prepared by applying pressure at the set temperature (I) and after alignment at 1000°C (II)

Procedure	Composition	Hot-pressing conditions			Relative density (%)
		Temp. (°C)	Pressure (MPa)	Time (min)	
I	C20	1750	25	30	97.3
I	C30	1750	25	45	91.8
II	C20	1700	27	60	98.8
II	C30	1700	27	60	97.5

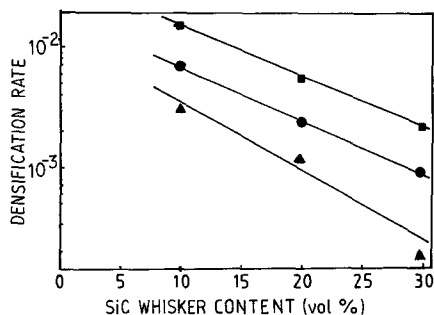


Figure 16 Plot of densification rate at $\rho =$ (■) 0.75, (●) 0.8, (▲) 0.85 against SiC whisker content.

the composites. The MgO additive can effectively promote the densification of the composite and inhibit abnormal grain growth. High pressure is required to achieve substantial densification prior to grain growth. Kinetic studies suggest that densification in the intermediate stage of hot pressing is controlled by the boundary-diffusion mechanism, and that the densification rate decreases dramatically with SiC whisker content in an exponential relationship.

References

1. G. C. WEI and P. F. BECHER, *Amer. Ceram. Soc. Bull.* **64** (1985) 298.
2. R. LUNDBERG *et al.*, *Composites* **18** (1987) 125.
3. J. HOMENY, W. L. VAUGHN and M. K. FERBER, *Amer. Ceram. Soc. Bull.* **66** (1987) 333.

4. J. R. PORTER, F. F. LANGE and A. H. CHOKSHI, *ibid.* **66** (1987) 343.
5. M. D. SACKS, H. LEE and O. E. ROJAS, *J. Amer. Ceram. Soc.* **71** (1988) 370.
6. T. N. TIEGS and P. F. BECHER, *Amer. Ceram. Soc. Bull.* **66** (1987) 339.
7. R. F. ADAMS, "Slip Cast Ceramics", in "High Temperature Oxide Ceramics", Vol. 5, edited by A. M. Alper (Academic Press, New York, 1971) p. 145.
8. R. ZELLAN, "The Physics of Amorphous Solids" (Wiley, New York, 1983) pp. 183-6.
9. S. K. ROY and R. L. COBLE, *J. SA. Ceram. Soc.* **51** (1968) 1.
10. R. J. BROOK, "Controlled Grain Growth", in "Treatise on Materials Science and Technology", Vol. 9, edited by F. F. Y. Wang (Academic Press, New York, 1976) p. 331.
11. J. G. J. PEELAN, in "Sintering and Catalysis" (Plenum Press, New York, London, 1975) p. 443.
12. M. P. HARMER, PhD thesis, Leeds University (1980).
13. R. L. COBLE and R. SPRIGGS, in "Sintering and Related Phenomena", edited by G. C. Kuczynski, N. A. Norton and G. S. Gibbon (Gordon and Breach Science Publications, New York, London, 1965) p. 329.
14. C. HERRING, *J. Appl. Phys.* **21** (1950) 437.
15. R. L. COBLE, *ibid.* **34** (1963) 1679.
16. R. M. CANNON and R. L. COBLE, in "Deformation of Ceramic Materials", edited by R. C. Bradt and R. E. Tressler (Plenum Press, New York, 1975) pp. 61-100.

Received 19 July

and accepted 17 October 1989